Ultrasound-Promoted preparation and application of novel bifunctional core/shell Fe 3 O 4 @SiO 2 @PTS-APG as a robust catalyst in the expeditious synthesis of Hantzsch esters

Peyman Shakib
Iran University of Science and Technology
Mohammad G. Dekamin (mdekamin@iust.ac.ir)
Iran University of Science and Technology
Ehsan Valiey
Iran University of Science and Technology
Shahriar Karami
Iran University of Science and Technology

Article

Keywords: D− (−)-α-phenylglycine (APG), Green chemistry, Polyhydroquinolines (PHQs) and 1,4-dihydropyridines (1,4-DHPs), Ultrasonic radiation, Magnetic nanocatalyst, Synergistic effect

Posted Date: October 3rd, 2022

DOI: https://doi.org/10.21203/rs.3.rs-2109934/v1

Additional Declarations: No competing interests reported.

Version of Record: A version of this preprint was published at Scientific Reports on May 17th, 2023. See the published version at https://doi.org/10.1038/s41598-023-33990-7.

Abstract

In this work, D-(−)-α-phenylglycine (APG)-functionalized magnetic nanocatalyst (Fe_3O_4@SiO_2@PTS-APG) was designed and successfully prepared in order to implement the protocols of green chemistry for the synthesis of polyhydroquinoline (PHQ) and 1,4-dihydropyridine (1,4-DHP) derivatives under ultrasonic radiation in EtOH. After preparing the nanocatalyst and confirming its structure by different spectroscopic methods or techniques including Fourier transform infrared (FT-IR) spectroscopy, energy-dispersive X-ray spectroscopy (EDS), field emission scanning electron microscopy (FESEM), X-ray diffraction (XRD), vibrating sample magnetometer (VSM) and thermal gravimetric analysis (TGA). Its performance under ultrasonic radiation and various conditions were examined. The yield of target derivatives was controlled under various conditions and it was found that it reaches more than 80% in just 10 min, which indicates the high performance of the nanocatalyst along with the synergistic effect of ultrasonic radiation. The structure of the products was identified by melting point as well as FT-IR and ^{1}H NMR spectroscopic methods. The Fe_3O_4@SiO_2@PTS-APG nanocatalyst is easily prepared from commercially available, lower toxicity and thermally stable precursors through a cost-effective, highly efficient and environmentally friendly procedure. The advantages of this method include simplicity of operation, reaction under mild conditions, use of environmental radiation sources, obtaining pure products with high efficiency in the shortest time without using a tedious path which is all in the shadow of green chemistry. Finally, a reasonable mechanism is proposed for the preparation of polyhydroquinoline (PHQ) and 1,4-dihydropyridine (1,4-DHP) derivatives in the presence of Fe_3O_4@SiO_2@PTS-APG bifunctional magnetic nanocatalyst.

1. Introduction

It's been a long time; heterogeneous catalysts have been known and used as an effective and environmentally friendly agent for organic transformations and to prevent the production of by-products[1–6]. These catalysts have several advantages including high selectivity, high turnover numbers (TON), and effortless optimization of catalytic activity, for example, by simply tuning ligand and metals in the case of metal complex catalyzed reactions[7, 8]. Various substrates are used to stabilize catalytic factors, which is one of the most important substrates is magnetite (Fe_3O_4)[5, 9]. Magnetite is an ideal oxide substrate that has a very active surface to absorb or stabilize metals and ligands and on the other hand, it can be easily separated and recyclable by applying external magnetic fields from the reaction medium[10–15]. Although the Fe_3O_4 magnetic nanoparticles (MNPs) are attracted to their unique properties, such as low price, broad availability, high surface area, Increased reaction rate by local heat through induction, thermal stability, low toxicity, easy separation of the reaction mixture by the application of an external magnetic field, a good potential for consolidation of different groups and excellent recycling capability, they are not stable under environmental conditions and are easily oxidized or dissolved in an acidic environment. In order to, overcome these problems, silica is commonly used as a protective shell for the coating of Fe_3O_4 MNPs and a magnetic core-shell nanostructure (Fe_3O_4@SiO_2) is formed[16, 17]. Furthermore, silica prevents the agglomeration of Fe_3O_4 MNPs, and also the most surface

of silyl groups, it is possible to modify their surface by different functional groups. It should be noted that the silica shell has a high porosity, is suitable for compatibility with the environment, and is an inexpensive material[18, 19].

α-Amino acids are natural compounds that make proteins in living systems. However, they can be considered as bifunctional organocatalysts from a catalytic point of view to activate both nucleophilic and electrophilic centers of the substrates through their carboxylic acid (-COOH) and amino ($-NH_2$) functional groups with proper geometry, respectively[20]. On the other hand, the natural abundance of α-amino acids as well as their optic activity make them appropriate candidates for the preparation of nontoxic catalytic systems with proper biodegradability. Also, α-amino acids demonstrate low solubility in organic solvents and are pH-sensitive. Therefore, designing and preparation of catalytic systems using α-amino acid units would be very beneficial from a green chemistry perspective to be used in the chemical, pharmaceutical, food, biotechnology, medical industries. [21, 22]. The preparation of ionic liquids is another application of amino acids that can be mentioned[23, 24]. For example, a team of American researchers successfully synthesized three [EMIM][AA]-type of amino acid ionic liquids and immobilized them into nanoporous polymethylmethacrylate (PMMA) microspheres and used as robust sorbents for CO_2[25]. Other researchers have used amino acids as a modulator in the preparation of zirconium and hafnium metal-organic frameworks (MOFs)[26]. Selenium nanoparticles (SeNPs) is an element used in the treatment of cancer and their major forms are organic and inorganic[27–29]. On the other hand, SeNPs are unstable and their use is limited by agglomerated, so biomolecules are used to stabilize these nanoparticles[30]. Researchers have shown that the interaction of NH_3^+ amino acid groups with negatively charged SeNPs can lead to the stability of these nanoparticles (SeNPs@AAs). Therefore, amino acids not only lead to stability and prevent the agglomeration of SeNPs, but also affect their anti-cancer function and increase their biological activity. These characteristics and wide applications of AAs encouraged our research team to use them as a catalyst and to advance the process in the preparation and identification of some of the six-membered heterocyclic rings.

Heterocyclic compounds are highly regarded and mainly synthesized due to their wide range of biological activities[31]. These compounds are used as key frameworks for the development of many therapeutic agents and play a prominent role in medicinal chemistry[32]. One of the best methods for preparing these bioactive compounds is the use of multicomponent reactions (MCRs).[33] In these reactions (domino processes), several starting materials (more than two reactants) react simultaneously and in one step at the presence of a catalyst and produce the desired product[34–37]. Multi-component reactions have unique advantages, such as the production of complex and diverse products through the formation of several bonds during an operation, without the need to isolate and purify the intermediates with high efficiency and high selectivity in the shortest time, together with the high atomic economy, therefore, they prevent the production of side and waste products during the reaction[38–41]. Polyhydroquinoline (PHQ) and 1,4-dihydropyridine (1,4-DHP) derivatives are some of the most important and oldest multi-component reactions that were first reported in 1882 by a German chemist named Arthur Hanztsch[42–44]. These compounds, due to pharmacological and biological activities, include the treatment of

cardiovascular diseases such as high blood pressure (such as nicardipine, nifedipine, aponepidine, nimodipine, and depin, etc.) (Fig. 1)[45, 46], antiviral[47], antitumor[48], antimalarial[49], antibacterial[50], anti-cancer[51], blocked calcium channels[52] activities, as well as coenzyme NADH, have been widely considered for reducing carbonyl compounds and their derivatives[53] in recent decades. Therefore, according to the medical activities of the derivatives derived from the Hantzsch reaction to synthesize them, researchers to synthesize them used a variety of methods including the common heat[54], solar energy[55], and various catalytic systems such as molecular iodine[56], L- proline[57], magnetic nanoparticles Fe_3O_4[58], nanoparticles ZnO[59], polymers[60], Hy-zeolite[61]. Most of these processes suffer from disadvantages such as long reaction times, low yields, harsh conditions, high costs, feed high values, the use of hazardous catalysts, toxic and volatile solvents, and boring workup.

Over the past few decades, due to the energy crisis and environmental pollution, green chemistry has received a lot of attention[62]. The principles of green chemistry have led to the development of cleaner and milder processes, especially in chemical synthesis[63]. Sonochemistry and microwave-assisted chemistry are not only used to accelerate organic reactions but are also an environmentally friendly synthetic protocol, which we will discuss in the following[64, 65]:

Ultrasonic (US) radiation has recently emerged as a clean and green method to accelerate organic synthetic conversions[66, 67]. It generates high temperatures and pressures in a very short period of time. The main advantages of ultrasonic synthesis are high reaction rate, short reaction time, high efficiency, and mild reaction conditions[68, 69]. In fact, ultrasonic radiation initiates chemical reactions by creating sound cavities that are used to overcome molecular gravitational forces[70, 71]. The process of cavitation refers to the rapid growth and collapse of bubbles in a liquid in which a chemical reaction takes place inside and near the bubbles and has two main paths[72]. Energy consumption for partial heating is inseparable from any chemical process. Microwave (MW) radiation is one of the most desirable energy sources to overcome this problem. Compared to other conventional methods, synthesis by microwave radiation is a logical method in green chemistry that not only improves the reaction rate, efficiency, and reaction path but also reduces waste and conserves energy[73]. Microwave radiation often provides high selectivity, simplicity of operation, and optimal energy compared to traditional methods[64, 74]. The heat from microwave radiation is highly dependent on the dielectric properties of solutions compared to traditional heat, so compounds with a high dielectric constant tend to absorb microwave radiation compared to compounds with lower polarity[75]. According to the discussion and the mentality created in connection with green chemistry protocols, sonochemistry, and microwave-assisted chemistry techniques are known as promising tools and because of their quick and easy applications, high performance, and being environmentally friendly, they are able to expand the boundaries of green chemistry. Therefore, it has been considered by many chemists in recent years[76]. Therefore, due to the properties of heterogeneous catalysts, the properties and applications of AAs, MCRs, and Hanztsch derivatives, clean and new energy sources, and circumvention of environmental hazards, in order to achieve the goals of green chemistry, we were encouraged to prepare magnetic heterogeneous nanocatalyst for the synthesis of bio-active polyhydroquinoline (PHQ) and 1,4-dihydropyridine (1,4-DHP) derivatives. For this purpose,

we successfully placed D-(−)-α-phenylglycine as a catalytic agent by 3-Chloropropyltrimethoxysilane (CPTES) on the surface of magnetic nanoparticles (MNPs) coated with silica (Fe_3O_4@SiO_2@PTS-APG).

Then, by the aforementioned nanocatalyst, bioactive PHQ and 1,4-DHP derivatives were synthesized under ultrasonic wave irradiation in a short time with high efficiency in ethanol solvent through a one-pot four-component reaction (Fig. 2). In addition, the aforementioned catalyst can be recycled at least five times without significant loss of catalytic activity and used in the subsequent cycles of the reaction. In the end, a reaction mechanism has been proposed to prepare these biologically active derivatives.

2. Results And Discussion

2.1. Analysis and characterization of magnetic core-shell catalyst functionalized with D-(−)-α-phenylglycine

First, using Catalyst infrared spectroscopy (FT-IR) spectra, scanning electron microscope images (SEM), vibrating sample magnetometer (VSM), X-ray powder diffraction technique (XRD), energy-dispersive X-ray spectroscopy (EDX), and thermogravimetric analysis (TGA) the structure of the core-shell magnetic nanocatalysts functionalized with D-(−)-α-phenylglycine is discussed in the experimental section. The structure of the core-shell magnetic silica functionalized with D-(−)-α-phenylglycine (Fe_3O_4@SiO_2@PTS@APG) has been illustrated in the experimental section (Fig. 11).

2.1.1. FT-IR spectra of the Fe_3O_4@SiO_2@Pr-APG catalyst

In order to confirm the synthesis of core-shell magnetic nanocatalysts functionalized with D-(−)-α-phenylglycine (Fe_3O_4@SiO_2@PTS-APG), first, let's examine the FT-IR spectrum. Figure 3, part (a) shows the magnetite spectrum. In this figure, the 572 cm^{-1} absorption frequencies are related to the stretching vibration of the Fe-O-Fe bond, which is a characteristic of the Fe_3O_4 nanoparticle structure. The absorbance bands with the center of 1558 cm^{-1} and 3394 cm^{-1} are related to the bending and stretching vibrations of the adsorbed water molecules on Fe_3O_4 nanoparticles, respectively. In section (b), the absorption band at 440 cm-1 area is related to the bending vibration of the Si O Si bond, whereas the vibration peak in the 800 cm^{-1} regions is related to the symmetric stretching vibration of Si O Si bond. The asymmetric tensile peak of the Si O Si bond appears in the 1085 cm^{-1} region, that indicating successful fixation of the silica onto the magnetite. Part (c) of the diagram shows the magnetite coated with silica along with the linker, which is a strong absorption band in the 588 cm^{-1} regions related to the stretching vibration of the C Cl bond and the peak observed in the 1070 cm^{-1} region is attributed to the stretching vibration of the C O bond, which overlaps with the asymmetric tensile vibration of the Si O Si bond. Part (d) of the diagram shows the spectrum of catalysts functionalized with (D)-(-)-α-Aminophenylacetic acid, in addition to the magnetite and silica peaks, one can see the stretching vibration of the C H bond at 2877 cm^{-1}, and the stretching vibration of the C N bond at 1382 cm^{-1}, as

well as the absorption band at the peak characteristics of 3490 cm^{-1} and 1639 cm^{-1}, are attributed to acidic OH group and carbonyl acetic acid group, respectively, which confirm the functionality of the above catalyst (Fig. 3).

2.1.2. EDS study of the Fe_3O_4@SiO_2@PTS-APG catalyst

After functionalization of magnetic nanoparticles, elemental analysis was performed to investigate them and further confirm the presence of essential elements. The Energy-dispersive X-ray spectroscopy (EDS) results obtained are shown in Fig. 4. As can be seen, the catalyst consists of atoms C, N, and O. In addition, the absence of the chlorine atom and the presence of the nitrogen atom indicate that the amino acid has been replaced and stabilized on the surface of the magnetic nanoparticles.

2.1.3. Microscopic imaging study of the Fe_3O_4@SiO_2@PTS-APG catalyst

In order to investigate the structure, morphological properties, and size of nanoparticles, the desired sample surface was imaged by Field emission scanning electron microscopy (FESEM) technique. The FESEM images of the synthesized nanocatalyst are shown in Fig. 10. These images are taken in three scales of 2μm (Fig. 5a), 200 nm (Fig. 5b-c), and 500 nm (Fig. 5d). It can be clearly seen that the obtained images confirm the spherical morphology with non-smooth surface and mono-dispersion of the nanoparticles. These properties increase the surface area and activity of the nanocatalyst because the highly active areas of the catalyst are readily available. According to Fig. 5c, it is clear that nanoparticles have a specific pattern and their average particle size is less than 60 nm.

2.1.4. Vibrating sample magnetometer (VSM) analysis of the Fe_3O_4@SiO_2@PTS-APG catalyst

As discussed at the beginning of the article in the introduction, one of the important reasons for choosing magnetic nanoparticles as a substrate is their separation and easy recyclability by an external magnetic field from the reaction medium. This is due to the super magnetic properties of magnetic nanoparticles. Based on this, the magnetic properties of Fe_3O_4, Fe_3O_4 @ SiO_2 and Fe_3O_4 @ SiO_2 @ PTS-APG were determined by the vibrating sample magnetometer (VSM) technique at room temperature (Fig. 6). As can be seen, the magnetic values for Fe_3O_4, Fe_3O_4 @ SiO_2, and Fe_3O_4 @ SiO_2 @ PTS-APG are 75, 70, and 58 $amu.g^{-1}$, respectively. The reduction of magnetic properties for Fe_3O_4 @ SiO_2 and Fe_3O_4 @ SiO_2 @ PTS-APG compared to bare Fe_3O_4 confirms the formation of a thin layer of silica and its surface modification with propylene trialkoxysilane and the stabilization of D-(−)-α-phenylglycine in the next stages.

2.1.5. XRD study of the Fe_3O_4@SiO_2@PTS-APG catalyst

The X-ray diffraction (XRD) pattern of the Fe_3O_4@SiO_2@PTS-APG nanoparticles is shown in Fig. 6. According to the standard patterns of Fe_3O_4 (card. No JCPDS, 01-088-0315), Fe_3O_4 @ SiO_2 (card. No JCPDS, 01-082-1572) and D-(−)-α-phenylglycine (card. No JCPDS, 00-013-0988) is fully compatible with nanocomposites. The diffraction signals (2θ) at 25, 28, and 31 correspond to D-(−)-α-phenylglycine, which confirms its stabilization on silica-coated magnetic nanoparticles.

2.1.6. Thermogravimetric analysis (TGA) of the Fe_3O_4@SiO_2@PTS-APG catalyst

In order to investigate the thermal stability of the hybrid organosilica nanocatalyst, thermogravimetric analysis (TGA) analysis was performed under N_2 atmosphere from 50 to 1000°C, which is discussed below. The total weight loss of the nanocatalyst was about 14% (Fig. 8). As can be seen, initially with a gradual increase in temperature to 95°C, a slight increase in the weight of the nanocatalyst is observed, which is due to the absorption of moisture by its hot surface. The first weight loss of about 100°C is related to adsorbed water or residual organic solvents in the nanocatalyst. At higher temperatures of about 150°C as well as 600 – 470°C, the organic components and the silica coating are decomposed or dehydrated, respectively. Finally, at temperatures above 600°C, a gradual decrease in weight is observed, which is related to dehydration of the magnetic component.

2.2. Optimization of reaction

In order to optimize the reaction conditions, a wide range of different organic solvents with the different power of ultrasonic radiation and various amounts of catalyst were investigated for the synthesis of polyhydroquinoline derivatives through a one-pot four-component reaction of 4-(dimethylamino)benzaldehyde (**1a**), ammonium acetate (**2**), ethyl acetoacetate (**3**), dimedone (**4**). In order to improve the synthesis of polyhydroquinoline derivatives and choose the best reaction conditions, a systematic study of these heterocyclic compounds was accomplished with a one-pot four-component reaction. thus 4-(dimethylamino)benzaldehyde (**1a**), ammonium acetate (**2**), ethyl acetoacetate (**3**), dimedone (**4**) as a model reaction in the presence of different organic solvents, in the variation of ultrasonic radiation power and diverse amounts of catalyst by several times were investigated, herein, the results of this study are summarized in Table 1. As shown in Table 1, the reaction in the absence of the catalyst under different conditions gives a very unfavorable yield (Table 1, entry 1). However, in the presence of the catalyst and various organic solvents, the product is formed with different yields (Table 1, entries 2–6), which among them, EtOH as the aprotic polar solvent has the best effect on reaction efficiency (Table 1, entry 2).

After determining the appropriate solvent, the rate of ultrasonic radiation power on the catalyst performance was investigated. It was observed that by increasing the ultrasonic radiation power from 75 to 80 W the rate of yield increases (Table 1, entries 6 and 7), and also from 80 to 85 W, the time decreases and yield rises (Table 1, entries 7 and 8), however, with an increase in ultrasonic radiation power to 90 W, there was no observed change in the time and efficiency of the reaction (Table 1, entry 9). These results

indicate that ultrasonic radiation power influences the time and reaction efficiency and therefore 85 W was chosen as the optimal radiation power. Finally, the effective amount of the catalyst on the reaction efficiency was investigated, which is considered to be 10 mg of catalyst as the optimal amount for the reaction (Table 1, entry 14). In general, the best conditions for this reaction are to synthesize (**5a**) using 10 mg of catalyst in the EtOH as a green solvent for 20 minutes (Table 1, entry 14).

After optimizing the reaction conditions, several polyhydroquinoline derivatives were synthesized at optimal conditions, and the results are summarized in Table 2. As shown in Table 2, substituted aldehydes containing electron-donating or electron-withdrawing groups produce excellent yields from the corresponding products.

Considering the satisfactory results obtained in the synthesis of polyhydroquinoline derivatives, the use of this catalyst for the synthesis of 1,4-dihydropyridine derivatives was investigated under optimum conditions (EtOH as a solvent and 85 W supersonic radiation power). In this study, 4-Chlorobenzaldehyde (**1a**), ammonium acetate (**2**), ethyl acetoacetate (**3**) were used as a reaction pattern for synthesis (**6a**) and the results are summarized in Table 3. Therefore, the best result is obtained with 10 mg of catalyst in the EtOH environment under ultrasonic radiation (Table 3, entry 6), accordingly, some 1,4-dihydropyridine derivatives were synthesized, the results of which are summarized in Table 4.

2.3. Mechanism of reaction

According to the structure and acidic and basic sites of the Fe_3O_4@SiO_2@PTS-APG MNPs and also the study of various literature[83, 84], a rational mechanism for the formation of polyhydroquinolines derivatives is proposed through the Hantzch reaction in the presence of nanocatalyst of Fe_3O_4@SiO_2@PTS-APG (Fig. 9).

Accordingly, these compounds can be synthesized in several steps so that the mechanism can proceed through path A or B. In the presence of catalytic acidic and basic sites, enamine cyclization occurs to the enone product. Based on route A, initially occurs a catalyzed Knoevenagel coupling reaction by acidic and basic catalyst sites between the derivatives of aldehydes and the enol form of dimedone and the intermediate (**i**) is formed, on the other side of the catalytic cycle, activated β-ketoester (by nanocatalyst) with ammonia released from NH_4OAC enamine (**ii**) gives. Subsequently, by catalyzed Michael addition by the catalyst between the intermediate species (**i**) and (**ii**), then cyclization leads to the formation of polyhydroquinoline derivatives. Route B is similar to path A, but with the difference that the Koevenagel reaction occurs between activated β-ketoester and the aldehyde derivatives species, which the (**iii**) and (**iv**) intermediates carried out Michael addition and then cyclization and formed polyhydroquinolines (PHQs) derivatives. On the other hand, this mechanism can also be used to synthesize 1,4-dihydropyridine (1,4-DHP) derivatives.

2.4. Comparison of the catalytic activity of Fe_3O_4@SiO_2@PTS-APG NPs with other catalytic systems

To compare the performance and activity of the Fe_3O_4@SiO_2@PTS-APG NPs compared to other previously reported catalysts, several products from the PHQ and 1,4-DHP derivatives randomly were selected and compared the reaction conditions for their synthesis with the results obtained by other previous methods and the results are summarized in Table 5. As shown in Table 5, our catalyst as an efficient nanocatalyst shows better results than other catalysts listed in Table 1 in terms of yields and reaction time. In summary, compared with other methods combination of synthesized nanocatalyst and ultrasonic waves has advantages, such as excellent yield, high selectivity, short reaction time, and mild reaction conditions.

2.5. Reusability of the Fe_3O_4@SiO_2@PTS-APG NPs

The catalyst recovery capability for chemical reactions is one of the most important advantages of catalysts and an important parameter that makes them suitable for industrial applications. Therefore, to investigate the capability of recovering the catalyst, it was easily separated from the reaction mixture by applying an external magnetic field and washed with EtOH, then dried in an oven at 70°C for 2h. The catalyst was used for subsequent experiments up to 6 times under the same reaction conditions. The catalyst recovery capability in product synthesis 5b and 6a under optimized reaction conditions (Table 1, entry 14, and Table 3, entry 6, respectively) were studied as reaction models. According to Fig. 10, it can be concluded that this heterogeneous catalyst can be used at least 6 times without loss of significant catalytic activity.

3. Experimental

3.1. Materials and methods

All the chemicals and solvents were purchased from Merck and used without further purification. The progress of reactions, as well as the purity, were checked using F254 silica-gel pre-coated TLC plates with n-hexane and ethyl acetate (1:1, v/v) as eluent. The melting points were determined on a Buchi melting point apparatus and are uncorrected. IR spectra were recorded on a Perkin Elmer FT-IR spectrophotometer using KBr pellets in the range of 399–4490 cm^{-1}. ^1H NMR spectra were recorded on a Bruker 500 MHz for samples in $CDCL_3$, as a solvent, at ambient temperature. Ultrasonication was performed in a BANDELIN ultrasonic HD 3200 instrument with probe model US 70/T with a diameter of 6 mm that was immersed directly into the reaction mixture. A National microwave oven, model no. NN-K571MF (1000 W), was used for microwave-assisted reactions. Scanning electron microscopy (SEM) images were obtained on an EM 3200 instrument operated at 30kv accelerating voltage. Magnetization measurements were carried out on a BHV-55 vibrating sample magnetometer (VSM). The curve obtained from thermogravimetric analysis (TGA) was recorded in the air using a Bahr company STA 504 instrument. Energy- dispersive X-ray (EDX) analysis was carried out using a FESEM-SIGM (German) instrument.

3.2. Preparation of magnetite (Fe_3O_4) nanoparticles (NPs) coated with silica (Fe_3O_4@ SiO_2)

In brief, 4.82 gr of $FeCl_3.6H_2O$ and 2.25 gr of $FeCl_2.4H_2O$ were dissolved in 40 mL deionized water at 80°C for 20 min under a nitrogen atmosphere with vigorous stirring. Then, 10 mL of aqueous NH_3 (25%) was added into the solution and was vigorously stirred at 70°C for 1h. The color of the bulk solution turned from orang to black immediately. The precipitated Fe_3O_4 nanoparticles were separated from the solution using a magnet and washed several times with deionized water and ethanol until the pH value reached the neutral positions, and left to dry in the air. Then 1.0 gr synthesized Fe_3O_4 NPs were mixed with 40 mL ethanol and 15 mL deionized water by ultrasonic treatment for 20 min. 1.2 mL of TEOS (silica precursor) was added to the mixture and sonicated for another 15 min and then 1.2 mL aqueous ammonia was added slowly under mechanical stirrer at 30°C. After 12h, the silica-coated magnetic nanoparticles were entered, washed several times with ethanol and distilled waters, and dried at 50°C.

3.3. Preparation of modified silica-coated magnetite NPs (Fe_3O_4@SiO_2@CPTS)

One gram of silica-coated Fe_3O_4 (Fe_3O_4@ SiO_2) nanoparticles were suspended in 40 mL toluene with sonication and then functionalized using 1 mL chloropropyltriethoxysilane (CPTES) by refluxing at 110°C for 24 h under nitrogen atmosphere. The resulting solid was collected and washed several times by ethanol and then dried at 80°C.

3.4. Immobilization of the D-(−)-α-phenylglycine (APG) on the surface of modified silica-coated magnetite NPs (Fe_3O_4@ SiO_2@PTS-APG)

One gram of Fe_3O_4@SiO_2@CPTS Powder was suspended in 40 mL ethanol and then 1.0 gr of D-(−)-α-phenylglycine was added into the solution and subsequently, the reaction mixture was refluxed at 70°C for 24 h. The resultant solid sample was separated using a magnet and washed several times with ethanol. Finally, the sample dried under vacuum at 80°C for 24h.

3.5. General procedure for the synthesis of PHQ and 1,4-DHPs derivatives

A mixture of aldehyde derivatives (1.0 mmol), ammonium acetate (1.0 mmol), ethyl acetoacetate (1.0 mmol), dimedone (1.0 mmol), the catalyst (10.0 mg), and ethanol (5.0 mL) were charged in a round-bottomed Flask and then contents were irradiated by an ultrasonic probe sonicator under conditions for times indicated in Table 2 and the formation of the products was monitored by TLC. In order to synthesis of 1,4-DHPs derivatives, the catalyst (10.0 mg), aldehyde derivatives (1.0 mmol), ammonium acetate (1.0 mmol), ethyl acetoacetate (2.0 mmol), and ethanol (2.0 mL) was placed into a round-bottomed and then irradiated by an ultrasonic probe sonicator under conditions for times indicated in Table 4 and the progress of the reaction was monitored by TLC. After the reaction was complete the catalyst was recovered by an external magnet and the pure product was obtained after recrystallization from EtOH-water. The chemical structure of the known materials was confirmed by comparing their melting points

and obtaining their FTIR and ^{1}HNMR spectra with the data reported in the sources. Examples of physical and spectral information of compounds 5a and 6a are given in Table 6.

4. Conclusion

In this work, we have developed a robust and efficient bifunctional organocatalyst immobilized on the surface of modified silica-coated magnetite NPs for the preparation of different polyhydroquinoline (PHQ) and 1,4-dihydropyridine (1,4-DHP) derivatives through the multicomponent reaction of Hantzsch condensation under ultrasonic irradiation in EtOH as a solvent. Various energy sources were used to synthesize these derivatives, among which ultrasonic triumphed. Indeed, ultrasonic waves with a synergistic effect combined with nanocatalyst accelerated the reaction rate. This method has significant advantages over other commonly used methods, which include the lack of use of harmful solvents, high efficiency, short reaction time, environmentally friendly, and inexpensive. Also, the synthesized heterogeneous nanocatalyst showed good recycling capability so that it can be easily recycled at least 5 times without loss of catalytic activity and used in subsequent performances. The principles of green chemistry were fulfilled by the use of recyclable catalysts, green solvent and efficient energy source, all of which are environmentally friendly.

Declarations

Availability of data and materials

All data generated or analyzed during this study are included in this published article [and its supplementary information files].

Acknowledgements

We are grateful for the financial support from The Research Council of Iran University of Science and Technology (IUST), Tehran, Iran (Grant No 160/20969) for their support. We would also like to acknowledge the support of The Iran Nanotechnology Initiative Council (INIC), Iran.

Contributions

P.Sh. worked on the topic, as his MSc thesis, and prepared the initial draft of the manuscript. Prof. M.G.D. is the supervisor of Mr. P.Sh., Mr. E.V. and Mr. Sh.K., as his MSc. and Ph.D students. Also, he edited and revised the manuscript completely. Mr. E.V. worked closely with P.Sh. for doing experiments and interpreting of the characterization data. Mr. Sh.K. also worked closely with P.Sh.for doing some experiments and drawing of graphs.

Ethics declarations

Competing interests

The authors declare no competing interests.

References

1. H. Wu, Z. Wang, L. Tao, The Hantzsch reaction in polymer chemistry: synthesis and tentative application, Polymer Chemistry, 8 (2017) 7290-7296.
2. Q. Zhang, Y. Zhao, B. Yang, C. Fu, L. Zhao, X. Wang, Y. Wei, L. Tao, Lighting up the PEGylation agents via the Hantzsch reaction, Polymer Chemistry, 7 (2016) 523-528.
3. M. Rezaie, M. Dinari, A.N. Chermahini, M. Saraji, A. Shahvar, Preparation of kapa carrageenan-based acidic heterogeneous catalyst for conversion of sugars to high-value added materials, International Journal of Biological Macromolecules, 165 (2020) 1129-1138.
4. M. Sam, M.G. Dekamin, Z. Alirezvani, Dendrons containing boric acid and 1, 3, 5-tris (2-hydroxyethyl) isocyanurate covalently attached to silica-coated magnetite for the expeditious synthesis of Hantzsch esters, Scientific reports, 11 (2021) 1-21.
5. H. Veisi, B. Karmakar, T. Tamoradi, R. Tayebee, S. Sajjadifar, S. Lotfi, B. Maleki, S. Hemmati, Bio-inspired synthesis of palladium nanoparticles fabricated magnetic Fe3O4 nanocomposite over Fritillaria imperialis flower extract as an efficient recyclable catalyst for the reduction of nitroarenes, Scientific Reports, 11 (2021) 1-15.
6. X. Chen, Y. Peng, X. Han, Y. Liu, X. Lin, Y. Cui, Sixteen isostructural phosphonate metal-organic frameworks with controlled Lewis acidity and chemical stability for asymmetric catalysis, Nature communications, 8 (2017) 1-9.
7. V. Polshettiwar, R. Luque, A. Fihri, H. Zhu, M. Bouhrara, J.-M. Basset, Magnetically recoverable nanocatalysts, Chemical reviews, 111 (2011) 3036-3075.
8. X. Cui, A.-E. Surkus, K. Junge, C. Topf, J. Radnik, C. Kreyenschulte, M. Beller, Highly selective hydrogenation of arenes using nanostructured ruthenium catalysts modified with a carbon–nitrogen matrix, Nature communications, 7 (2016) 1-8.
9. Z. Alirezvani, M.G. Dekamin, E. Valiey, Cu (II) and magnetite nanoparticles decorated melamine-functionalized chitosan: A synergistic multifunctional catalyst for sustainable cascade oxidation of benzyl alcohols/Knoevenagel condensation, Scientific reports, 9 (2019) 1-12.
10. J.S. Ghomi, S. Zahedi, Novel ionic liquid supported on Fe3O4 nanoparticles and its application as a catalyst in Mannich reaction under ultrasonic irradiation, Ultrasonics Sonochemistry, 34 (2017) 916-923.
11. C.A. Mak, M.A. Pericas, E. Fagadar-Cosma, Functionalization of A3B-type porphyrin with Fe3O4 MNPs. Supramolecular assemblies, gas sensor and catalytic applications, Catalysis Today, 306 (2018) 268-275.
12. M. Neamtu, C. Nadejde, V.-D. Hodoroaba, R.J. Schneider, L. Verestiuc, U. Panne, Functionalized magnetic nanoparticles: Synthesis, characterization, catalytic application and assessment of toxicity, Scientific reports, 8 (2018) 1-11.

13. Y. Zhou, S. Yuan, Q. Liu, D. Yan, Y. Wang, L. Gao, J. Han, H. Shi, Synchronized purification and immobilization of his-tagged β-glucosidase via Fe3O4/PMG core/shell magnetic nanoparticles, Scientific Reports, 7 (2017) 1-11.
14. F. Alnadari, Y. Xue, L. Zhou, Y.S. Hamed, M. Taha, M.F. Foda, Immobilization of β-glucosidase from Thermatoga maritima on chitin-functionalized magnetic nanoparticle via a novel thermostable chitin-binding domain, Scientific reports, 10 (2020) 1-12.
15. Q. Li, C.W. Kartikowati, S. Horie, T. Ogi, T. Iwaki, K. Okuyama, Correlation between particle size/domain structure and magnetic properties of highly crystalline Fe3O4 nanoparticles, Scientific reports, 7 (2017) 1-7.
16. K.V. Ranganath, F. Glorius, Superparamagnetic nanoparticles for asymmetric catalysis—a perfect match, Catalysis Science & Technology, 1 (2011) 13-22.
17. S. Karami, M.G. Dekamin, E. Valiey, P. Shakib, DABA MNPs: a new and efficient magnetic bifunctional nanocatalyst for green synthesis of biologically active pyrano [2, 3-c] pyrazole and benzylpyrazolyl coumarin derivatives, New Journal of Chemistry, (2020).
18. M. Shao, F. Ning, J. Zhao, M. Wei, D.G. Evans, X. Duan, Preparation of Fe3O4@ SiO2@ layered double hydroxide core–shell microspheres for magnetic separation of proteins, Journal of the American Chemical Society, 134 (2012) 1071-1077.
19. P. Wang, H. Liu, J. Niu, R. Li, J. Ma, Entangled Pd complexes over Fe 3 O 4@ SiO 2 as supported catalysts for hydrogenation and Suzuki reactions, Catalysis Science & Technology, 4 (2014) 1333-1339.
20. M.G. Dekamin, Z. Karimi, Z. Latifidoost, S. Ilkhanizadeh, H. Daemi, M.R. Naimi-Jamal, M. Barikani, Alginic acid: A mild and renewable bifunctional heterogeneous biopolymeric organocatalyst for efficient and facile synthesis of polyhydroquinolines, International journal of biological macromolecules, 108 (2018) 1273-1280.
21. A. Bossi, M. Cretich, P.G. Righetti, Production of D-phenylglycine from racemic (D, L)-phenylglycine via isoelectrically-trapped penicillin G acylase, Biotechnology and bioengineering, 60 (1998) 454-461.
22. D. Grishin, D. Zhdanov, M. Pokrovskaya, N. Sokolov, D-amino acids in nature, agriculture and biomedicine, All Life, 13 (2020) 11-22.
23. G.-h. Tao, L. He, W.-s. Liu, L. Xu, W. Xiong, T. Wang, Y. Kou, Preparation, characterization and application of amino acid-based green ionic liquids, Green Chemistry, 8 (2006) 639-646.
24. Y.-Y. Jiang, G.-N. Wang, Z. Zhou, Y.-T. Wu, J. Geng, Z.-B. Zhang, Tetraalkylammonium amino acids as functionalized ionic liquids of low viscosity, Chemical communications, (2008) 505-507.
25. X. Wang, N.G. Akhmedov, Y. Duan, D. Luebke, B. Li, Immobilization of amino acid ionic liquids into nanoporous microspheres as robust sorbents for CO 2 capture, Journal of Materials Chemistry A, 1 (2013) 2978-2982.
26. R.J. Marshall, C.L. Hobday, C.F. Murphie, S.L. Griffin, C.A. Morrison, S.A. Moggach, R.S. Forgan, Amino acids as highly efficient modulators for single crystals of zirconium and hafnium metal–organic frameworks, Journal of Materials Chemistry A, 4 (2016) 6955-6963.

27. R. Stone, A medical mystery in middle China, American Association for the Advancement of Science, 2009.
28. G.V. Kryukov, S. Castellano, S.V. Novoselov, A.V. Lobanov, O. Zehtab, R. Guigó, V.N. Gladyshev, Characterization of mammalian selenoproteomes, Science, 300 (2003) 1439-1443.
29. J. Wang, X. Yang, A. Bao, X. Liu, J. Zeng, X. Liu, J. Yao, J. Zhang, Z. Lei, Microwave-assisted synthesis, structure and anti-tumor activity of selenized Artemisia sphaerocephala polysaccharide, International journal of biological macromolecules, 95 (2017) 1108-1118.
30. M. Gallego-Gallegos, L.E. Doig, J.J. Tse, I.J. Pickering, K. Liber, Bioavailability, toxicity and biotransformation of selenium in midge (Chironomus dilutus) larvae exposed via water or diet to elemental selenium particles, selenite, or selenized algae, Environmental science & technology, 47 (2013) 584-592.
31. B. Banerjee, Recent developments on ultrasound-assisted one-pot multicomponent synthesis of biologically relevant heterocycles, Ultrasonics sonochemistry, 35 (2017) 15-35.
32. N. Kaur, Ultrasound-assisted green synthesis of five-membered O-and S-heterocycles, Synthetic Communications, 48 (2018) 1715-1738.
33. M.G. Dekamin, E. Kazemi, Z. Karimi, M. Mohammadalipoor, M.R. Naimi-Jamal, Chitosan: An efficient biomacromolecule support for synergic catalyzing of Hantzsch esters by CuSO4, International journal of biological macromolecules, 93 (2016) 767-774.
34. T.S. Saleh, T.M. Eldebss, H.M. Albishri, Ultrasound assisted one-pot, three-components synthesis of pyrimido [1, 2-a] benzimidazoles and pyrazolo [3, 4-b] pyridines: a new access via phenylsulfone synthon, Ultrasonics sonochemistry, 19 (2012) 49-55.
35. A.C. Boukis, K. Reiter, M. Frölich, D. Hofheinz, M.A. Meier, Multicomponent reactions provide key molecules for secret communication, Nature communications, 9 (2018) 1-10.
36. M. Koolivand, M. Nikoorazm, A. Ghorbani-Choghamarani, R. Azadbakht, B. Tahmasbi, Ni–citric acid coordination polymer as a practical catalyst for multicomponent reactions, Scientific reports, 11 (2021) 1-16.
37. N. Hussain-Khil, A. Ghorbani-Choghamarani, M. Mohammadi, A new silver coordination polymer based on 4, 6-diamino-2-pyrimidinethiol: synthesis, characterization and catalytic application in asymmetric Hantzsch synthesis of polyhydroquinolines, Scientific Reports, 11 (2021) 1-15.
38. Y. Gu, Multicomponent reactions in unconventional solvents: state of the art, Green Chemistry, 14 (2012) 2091-2128.
39. S. Gulati, R. Singh, S. Sangwan, Fruit juice mediated multicomponent reaction for the synthesis of substituted isoxazoles and their in vitro bio-evaluation, Scientific reports, 11 (2021) 1-16.
40. H. Ghafuri, Z. Tajik, N. Ghanbari, P. Hanifehnejad, Preparation and characterization of graphitic carbon nitride-supported l-arginine as a highly efficient and recyclable catalyst for the one-pot synthesis of condensation reactions, Scientific reports, 11 (2021) 1-14.
41. S. Saneinezhad, L. Mohammadi, V. Zadsirjan, F.F. Bamoharram, M.M. Heravi, Silver nanoparticles-decorated Preyssler functionalized cellulose biocomposite as a novel and efficient catalyst for the

synthesis of 2-amino-4H-pyrans and spirochromenes, Scientific reports, 10 (2020) 1-26.

42. S. Ghosh, F. Saikh, J. Das, A.K. Pramanik, Hantzsch 1, 4-dihydropyridine synthesis in aqueous ethanol by visible light, Tetrahedron Letters, 54 (2013) 58-62.
43. M. Li, Z. Zuo, L. Wen, S. Wang, Microwave-assisted combinatorial synthesis of hexa-substituted 1, 4-dihydropyridines scaffolds using one-pot two-step multicomponent reaction followed by a S-alkylation, Journal of combinatorial chemistry, 10 (2008) 436-441.
44. S.M. Ramish, A. Ghorbani-Choghamarani, M. Mohammadi, Microporous hierarchically Zn-MOF as an efficient catalyst for the Hantzsch synthesis of polyhydroquinolines, Scientific Reports, 12 (2022) 1-15.
45. P. Choudhury, P. Ghosh, B. Basu, Amine-functionalized graphene oxide nanosheets (AFGONs): an efficient bifunctional catalyst for selective formation of 1, 4-dihydropyridines, acridinediones and polyhydroquinolines, Molecular Diversity, 24 (2020) 283-294.
46. M. De Luca, G. Ioele, G. Ragno, 1, 4-Dihydropyridine Antihypertensive Drugs: Recent Advances in Photostabilization Strategies, Pharmaceutics, 11 (2019) 85.
47. A. Hilgeroth, Dimeric 4-Aryl-1, 4-dihydropyridines: development of a third class of nonpeptidic HIV-1 protease inhibitors, Mini Reviews in medicinal chemistry, 2 (2002) 235-245.
48. M. Kawase, A. Shah, H. Gaveriya, N. Motohashi, H. Sakagami, A. Varga, J. Molnar, 3, 5-Dibenzoyl-1, 4-dihydropyridines: synthesis and MDR reversal in tumor cells, Bioorganic & medicinal chemistry, 10 (2002) 1051-1055.
49. A. Ryckebusch, R. Deprez-Poulain, L. Maes, M.-A. Debreu-Fontaine, E. Mouray, P. Grellier, C. Sergheraert, Synthesis and in Vitro and in Vivo Antimalarial Activity of N-(7-Chloro-4-quinolyl)-1, 4-bis (3-aminopropyl) piperazine Derivatives, Journal of medicinal chemistry, 46 (2003) 542-557.
50. M. Zhang, A. Haemers, D. Vanden Berghe, S. Pattyn, W. Bollaert, I. Levshin, Quinolone antibacterials. 1. 7-(2-substituted-4-thiazolyl and thiazolidinyl) quinolones, Journal of heterocyclic chemistry, 28 (1991) 673-683.
51. S. Maiti, V. Sridharan, J.C. Menendez, Synthesis of a library of 5, 6-unsubstituted 1, 4-dihydropyridines based on a one-pot 4CR/elimination process and their application to the generation of structurally diverse fused nitrogen heterocycles, Journal of combinatorial chemistry, 12 (2010) 713-722.
52. M.S. Saddala, R. Kandimalla, P.J. Adi, S.S. Bhashyam, U.R. Asupatri, Novel 1, 4-dihydropyridines for L-type calcium channel as antagonists for cadmium toxicity, Scientific reports, 7 (2017) 45211.
53. M. Rueping, A.P. Antonchick, T. Theissmann, A highly enantioselective Brønsted acid catalyzed cascade reaction: organocatalytic transfer hydrogenation of quinolines and their application in the synthesis of alkaloids, Angewandte Chemie International Edition, 45 (2006) 3683-3686.
54. J. Sainani, A. Shah, V. Arya, Synthesis of 4-Aryl-1, 4, 5, 6, 7, 8-hexahydro-5-oxo-2, 7, 7-trimethyl-quinoline-3-carboxylates and Amides, ChemInform, 25 (1994) no-no.
55. R.A. Mekheimer, A.A. Hameed, K.U. Sadek, Solar thermochemical reactions: four-component synthesis of polyhydroquinoline derivatives induced by solar thermal energy, Green Chemistry, 10

(2008) 592-593.
56. S. Ko, M. Sastry, C. Lin, C.-F. Yao, Molecular iodine-catalyzed one-pot synthesis of 4-substituted-1, 4-dihydropyridine derivatives via Hantzsch reaction, Tetrahedron Letters, 46 (2005) 5771-5774.
57. N.N. Karade, V.H. Budhewar, S.V. Shinde, W.N. Jadhav, L-proline as an efficient organo-catalyst for the synthesis of polyhydroquinoline via multicomponent Hantzsch reaction, Letters in Organic Chemistry, 4 (2007) 16-19.
58. M. Nasr-Esfahani, S.J. Hoseini, M. Montazerozohori, R. Mehrabi, H. Nasrabadi, Magnetic Fe3O4 nanoparticles: efficient and recoverable nanocatalyst for the synthesis of polyhydroquinolines and Hantzsch 1, 4-dihydropyridines under solvent-free conditions, Journal of Molecular Catalysis A: Chemical, 382 (2014) 99-105.
59. M. Kassaee, H. Masrouri, F. Movahedi, ZnO-nanoparticle-promoted synthesis of polyhydroquinoline derivatives via multicomponent Hantzsch reaction, Monatshefte für Chemie-Chemical Monthly, 141 (2010) 317-322.
60. J.G. Breitenbucher, G. Figliozzi, Solid-phase synthesis of 4-aryl-1, 4-dihydropyridines via the Hantzsch three component condensation, Tetrahedron Letters, 41 (2000) 4311-4315.
61. B. Das, B. Ravikanth, R. Ramu, B.V. Rao, An efficient one-pot synthesis of polyhydroquinolines at room temperature using HY-zeolite, Chemical and pharmaceutical bulletin, 54 (2006) 1044-1045.
62. P. Gupta, S. Paul, Solid acids: Green alternatives for acid catalysis, Catalysis Today, 236 (2014) 153-170.
63. L. Zare, N.O. Mahmoodi, A. Yahyazadeh, M. Nikpassand, Ultrasound-promoted regio and chemoselective synthesis of pyridazinones and phthalazinones catalyzed by ionic liquid [bmim] Br/AlCl3, Ultrasonics sonochemistry, 19 (2012) 740-744.
64. Y. Wang, Q. Hou, M. Ju, W. Li, New developments in material preparation using a combination of ionic liquids and microwave irradiation, Nanomaterials, 9 (2019) 647.
65. B. Banerjee, Recent developments on ultrasound assisted catalyst-free organic synthesis, Ultrasonics sonochemistry, 35 (2017) 1-14.
66. P. Kumar, A. Kumar, K. Hussain, Iodobenzene diacetate (IBD) catalyzed an quick oxidative aromatization of Hantzsch-1, 4-dihydropyridines to pyridines under ultrasonic irradiation, Ultrasonics sonochemistry, 19 (2012) 729-735.
67. R. Pagadala, S. Maddila, S.B. Jonnalagadda, Eco-efficient ultrasonic responsive synthesis of pyrimidines/pyridines, Ultrasonics sonochemistry, 21 (2014) 472-477.
68. S.K. Maury, D. Kumar, A. Kamal, H.K. Singh, S. Kumari, S. Singh, A facile and efficient multicomponent ultrasound-assisted “on water” synthesis of benzodiazepine ring, Molecular Diversity, (2020) 1-12.
69. M. Nematpour, E. Rezaee, M. Jahani, S.A. Tabatabai, Ultrasound-assisted synthesis of highly functionalized benzo [1, 3] thiazine via Cu-catalyzed intramolecular CH activation reaction from isocyanides, aniline-benzoyl (acetyl) isothiocyanate adduct, Ultrasonics sonochemistry, 50 (2019) 1-5.

70. M.A. Dheyab, A.A. Aziz, M.S. Jameel, P.M. Khaniabadi, B. Mehrdel, Mechanisms of effective gold shell on Fe3O4 core nanoparticles formation using sonochemistry method, Ultrasonics sonochemistry, (2019) 104865.
71. E.V. Skorb, H. Moehwald, Ultrasonic approach for surface nanostructuring, Ultrasonics sonochemistry, 29 (2016) 589-603.
72. J.H. Bang, K.S. Suslick, Applications of ultrasound to the synthesis of nanostructured materials, Advanced materials, 22 (2010) 1039-1059.
73. E. Makhado, S. Pandey, J. Ramontja, Microwave assisted synthesis of xanthan gum-cl-poly (acrylic acid) based-reduced graphene oxide hydrogel composite for adsorption of methylene blue and methyl violet from aqueous solution, International journal of biological macromolecules, 119 (2018) 255-269.
74. W. Mortada, I. Kenawy, Y. Abou El-Reash, A. Mousa, Microwave assisted modification of cellulose by gallic acid and its application for removal of aluminium from real samples, International journal of biological macromolecules, 101 (2017) 490-501.
75. A.D. Hoz, A. Diaz-Ortiz, A. Moreno, Selectivity in organic synthesis under microwave irradiation, Current Organic Chemistry, 8 (2004) 903-918.
76. G. Chatel, R.S. Varma, Ultrasound and microwave irradiation: contributions of alternative physicochemical activation methods to Green Chemistry, Green Chemistry, 21 (2019) 6043-6050.
77. S.K. Singh, K.N. Singh, Glycine-catalyzed easy and efficient one-pot synthesis of polyhydroquinolines through Hantzsch multicomponent condensation under controlled microwave, Journal of Heterocyclic Chemistry, 47 (2010) 194-198.
78. G.D. Rao, S. Nagakalyan, G. Prasad, Solvent-free synthesis of polyhydroquinoline derivatives employing mesoporous vanadium ion doped titania nanoparticles as a robust heterogeneous catalyst via the Hantzsch reaction, RSC advances, 7 (2017) 3611-3616.
79. Q. Zhang, X.-M. Ma, H.-X. Wei, X. Zhao, J. Luo, Covalently anchored tertiary amine functionalized ionic liquid on silica coated nano-Fe 3 O 4 as a novel, efficient and magnetically recoverable catalyst for the unsymmetrical Hantzsch reaction and Knoevenagel condensation, RSC advances, 7 (2017) 53861-53870.
80. S. Zhaleh, N. Hazeri, M.R. Faghihi, M.T. Maghsoodlou, Chitosan: a sustainable, reusable and biodegradable organocatalyst for green synthesis of 1, 4-dihydropyridine derivatives under solvent-free condition, Research on Chemical Intermediates, 42 (2016) 8069-8081.
81. S. Taghavi Fardood, A. Ramazani, Z. Golfar, S.W. Joo, Green synthesis of Ni-Cu-Zn ferrite nanoparticles using tragacanth gum and their use as an efficient catalyst for the synthesis of polyhydroquinoline derivatives, Applied Organometallic Chemistry, 31 (2017) e3823.
82. L. Shiri, A. Ghorbani-Choghamarani, M. Kazemi, Synthesis and characterization of DETA/Cu (NO 3) 2 supported on magnetic nanoparticles: a highly active and recyclable catalyst for the solvent-free synthesis of polyhydroquinolines, Monatshefte für Chemie-Chemical Monthly, 148 (2017) 1131-1139.

83. S.K. Das, S. Mondal, S. Chatterjee, A. Bhaumik, N-rich Porous Organic Polymer as Heterogeneous Organocatalyst for the One-Pot Synthesis of Polyhydroquinoline Derivatives through the Hantzsch Condensation Reaction, ChemCatChem, 10 (2018) 2488-2495.
84. B.L. Li, A.G. Zhong, A.G. Ying, Novel SO3H-functionalized ionic liquids–catalyzed facile and efficient synthesis of polyhydroquinoline derivatives via hantzsch condensation under ultrasound irradiation, Journal of Heterocyclic Chemistry, 52 (2015) 445-449.
85. V. GOEL, A. BAJWAN, S. CHAUHAN, S. GOEL, An Efficient and Versatile Method for Synthesis of 1, 4-Dihydropyridines at Mild Reaction Conditions, Chemical Science, 7 (2018) 343-347.
86. H. Mirzaei, A. Davoodnia, Microwave assisted sol-gel synthesis of MgO nanoparticles and their catalytic activity in the synthesis of hantzsch 1, 4-dihydropyridines, Chinese journal of catalysis, 33 (2012) 1502-1507.
87. A. Debache, W. Ghalem, R. Boulcina, A. Belfaitah, S. Rhouati, B. Carboni, An efficient one-step synthesis of 1, 4-dihydropyridines via a triphenylphosphine-catalyzed three-component Hantzsch reaction under mild conditions, Tetrahedron Letters, 50 (2009) 5248-5250.
88. N. Taheri, F. Heidarizadeh, A. Kiasat, A new magnetically recoverable catalyst promoting the synthesis of 1, 4-dihydropyridine and polyhydroquinoline derivatives via the Hantzsch condensation under solvent-free conditions, Journal of Magnetism and Magnetic Materials, 428 (2017) 481-487.
89. H. Niaz, H. Kashtoh, J.A. Khan, A. Khan, M.T. Alam, K.M. Khan, S. Perveen, M.I. Choudhary, Synthesis of diethyl 4-substituted-2, 6-dimethyl-1, 4-dihydropyridine-3, 5-dicarboxylates as a new series of inhibitors against yeast α-glucosidase, European Journal of Medicinal Chemistry, 95 (2015) 199-209.
90. J.S. Yoo, T.J. Laughlin, J.J. Krob, R.S. Mohan, Bismuth (III) bromide catalyzed synthesis of polyhydroquinoline derivatives via the Hantzsch reaction, Tetrahedron Letters, 56 (2015) 4060-4062.
91. D.S. Rekunge, C.K. Khatri, G.U. Chaturbhuj, Sulfated polyborate: An efficient and reusable catalyst for one pot synthesis of Hantzsch 1, 4-dihydropyridines derivatives using ammonium carbonate under solvent free conditions, Tetrahedron Letters, 58 (2017) 1240-1244.
92. M. Safaiee, B. Ebrahimghasri, M.A. Zolfigol, S. Baghery, A. Khoshnood, D.A. Alonso, Synthesis and application of chitosan supported vanadium oxo in the synthesis of 1, 4-dihydropyridines and 2, 4, 6-triarylpyridines via anomeric based oxidation, New Journal of Chemistry, 42 (2018) 12539-12548.

Tables

Table 1 To 6 is available in the Supplementary Files section.

Figures

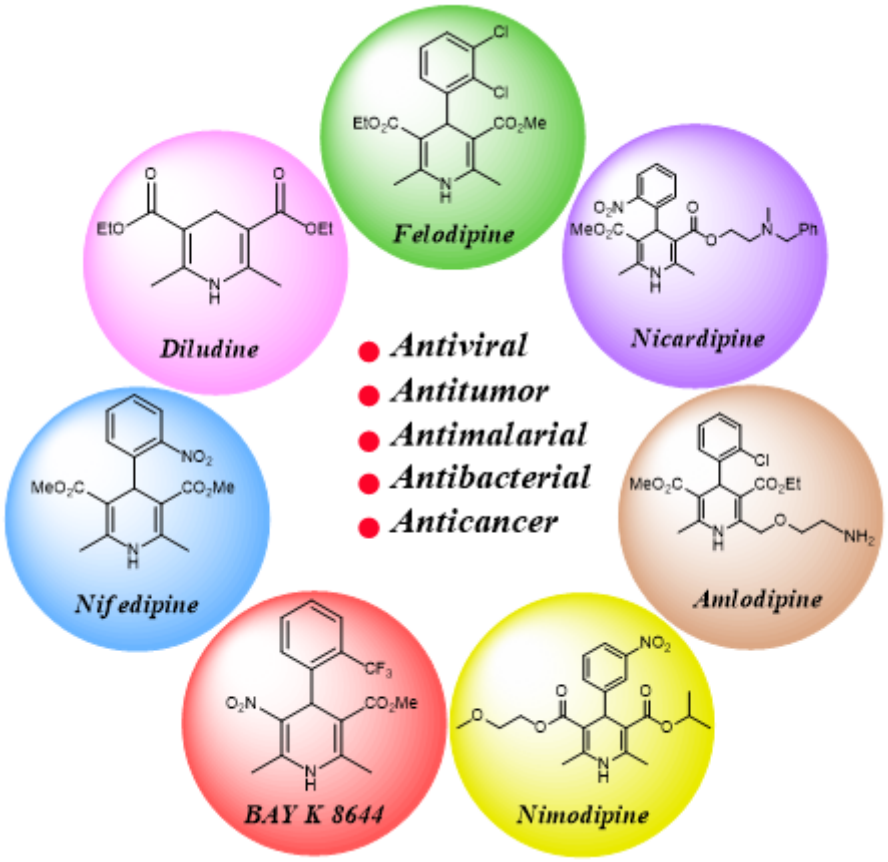

Figure 1

Some of the commercial biologically active polyhydroquinoline (PHQ) and 1,4-dihydropyridine (1,4-DHP) derivatives.

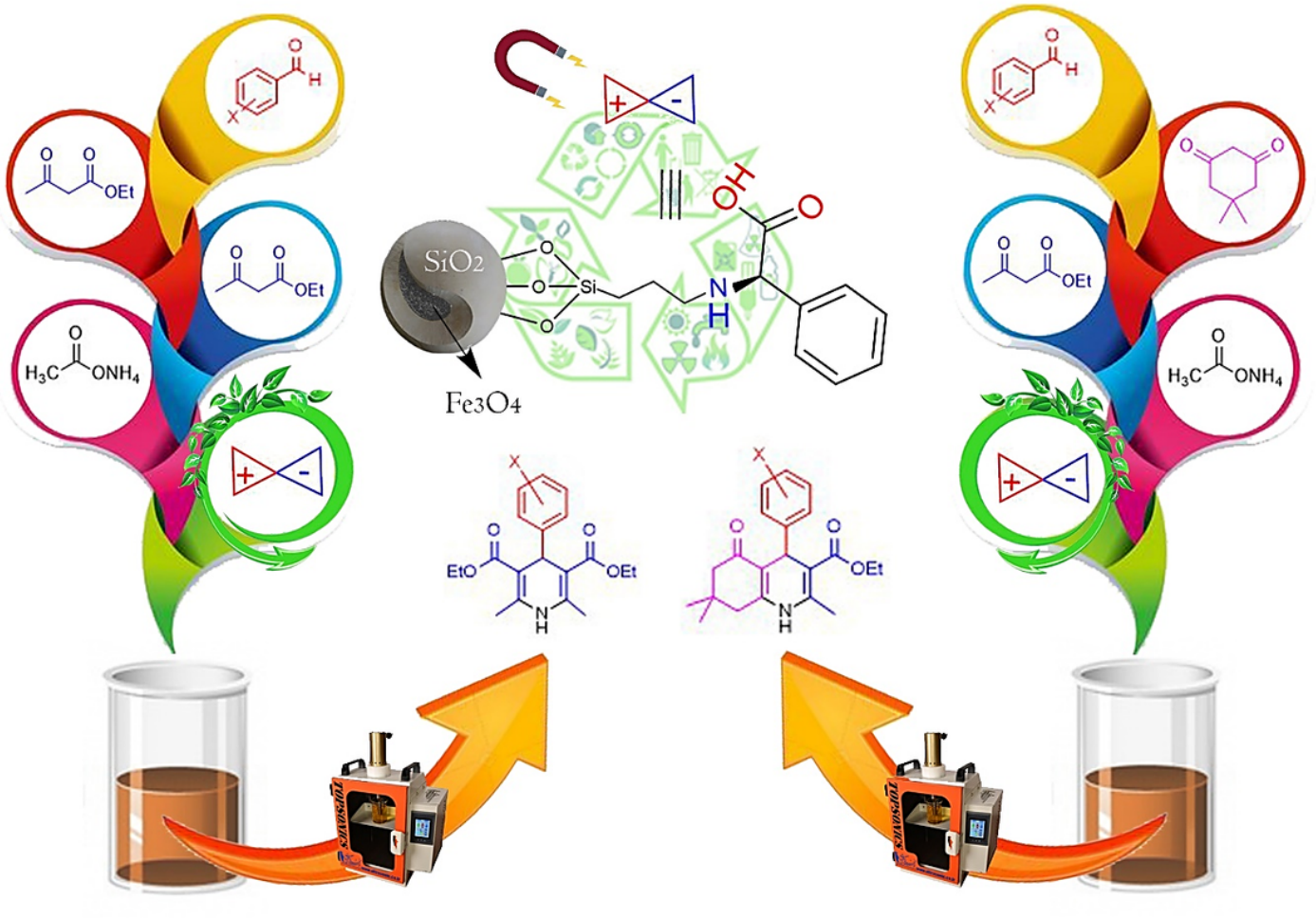

Figure 2

Synthesis of polyhydroquinoline (PHQ) 5 and 1,4-dihydropyridine (1,4-DHP) 6 derivatives catalyzed by Fe_3O_4@SiO_2@PTS-APG.

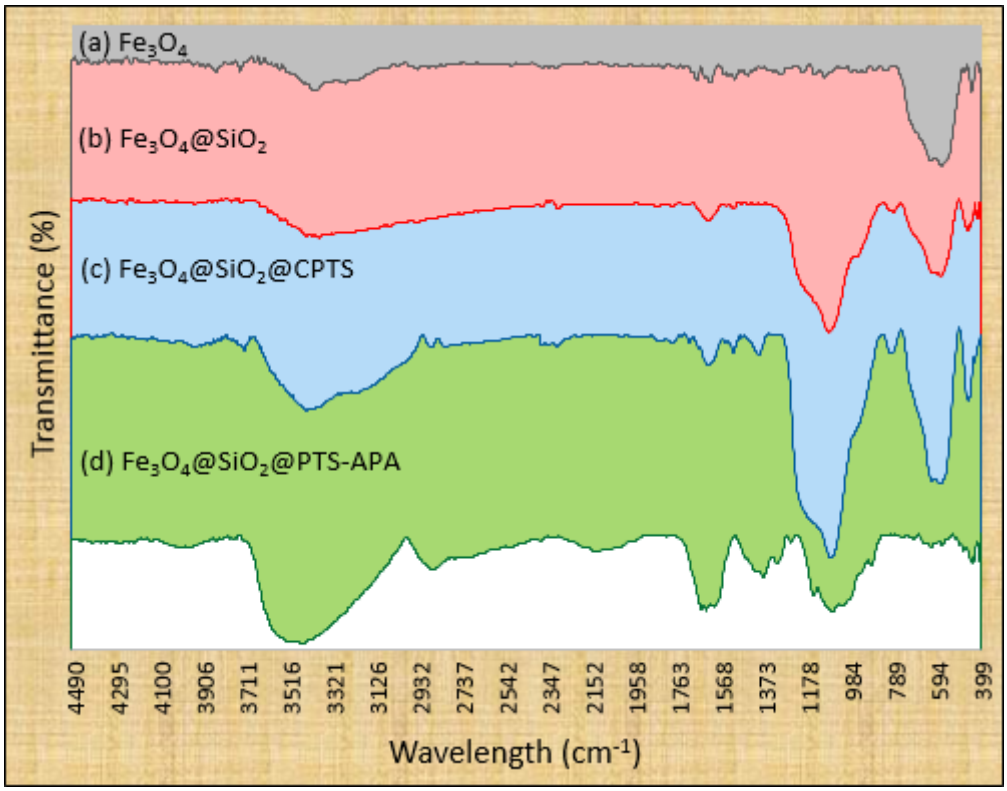

Figure 3

FT-IR spectra of (a) Fe_3O_4, (b) Fe_3O_4@SiO_2, (c) Fe_3O_4@SiO_2@CPTS, (d) Fe_3O_4@SiO_2@PTS-APG.

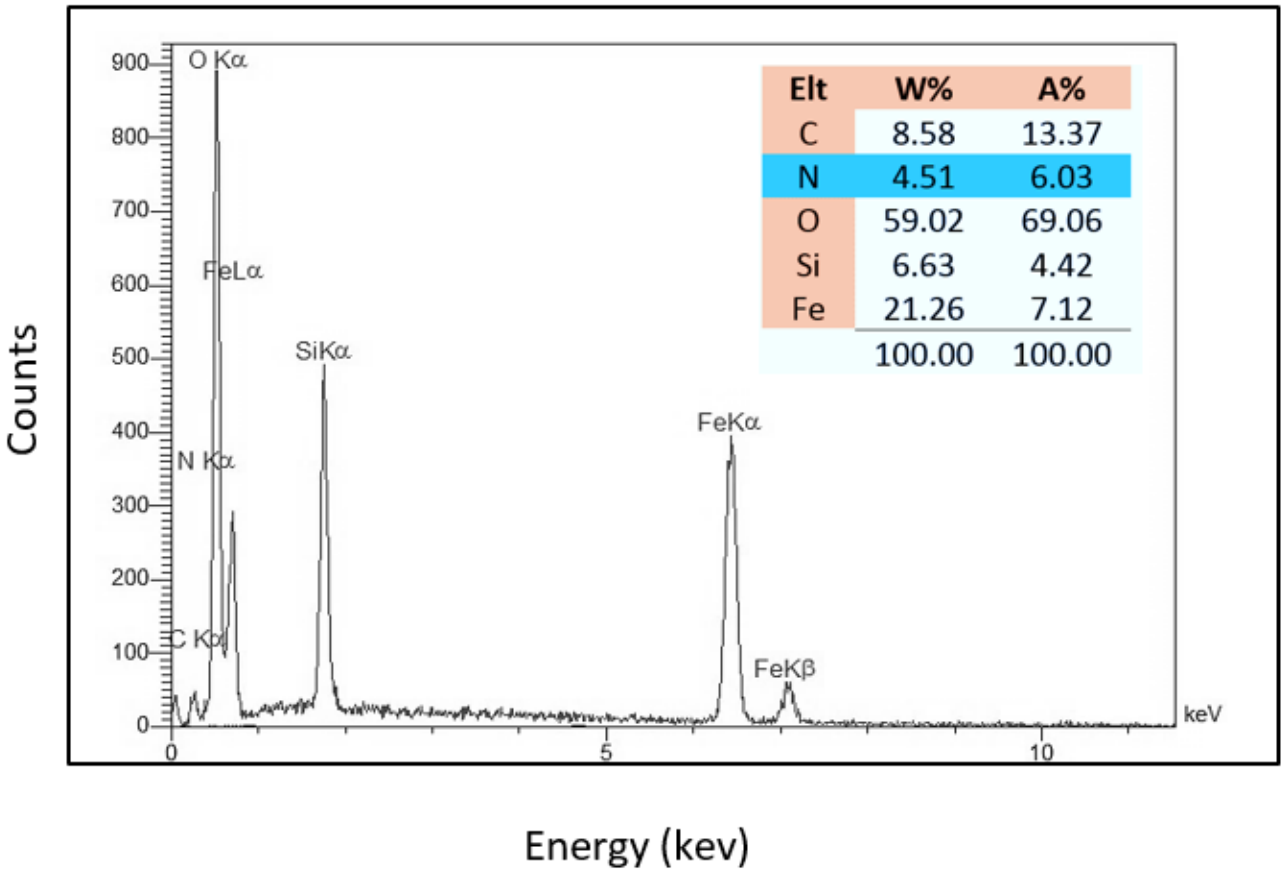

Elt	W%	A%
C	8.58	13.37
N	4.51	6.03
O	59.02	69.06
Si	6.63	4.42
Fe	21.26	7.12
	100.00	100.00

Figure 4

EDS of the Fe_3O_4@SiO_2@PTS-APG catalyst.

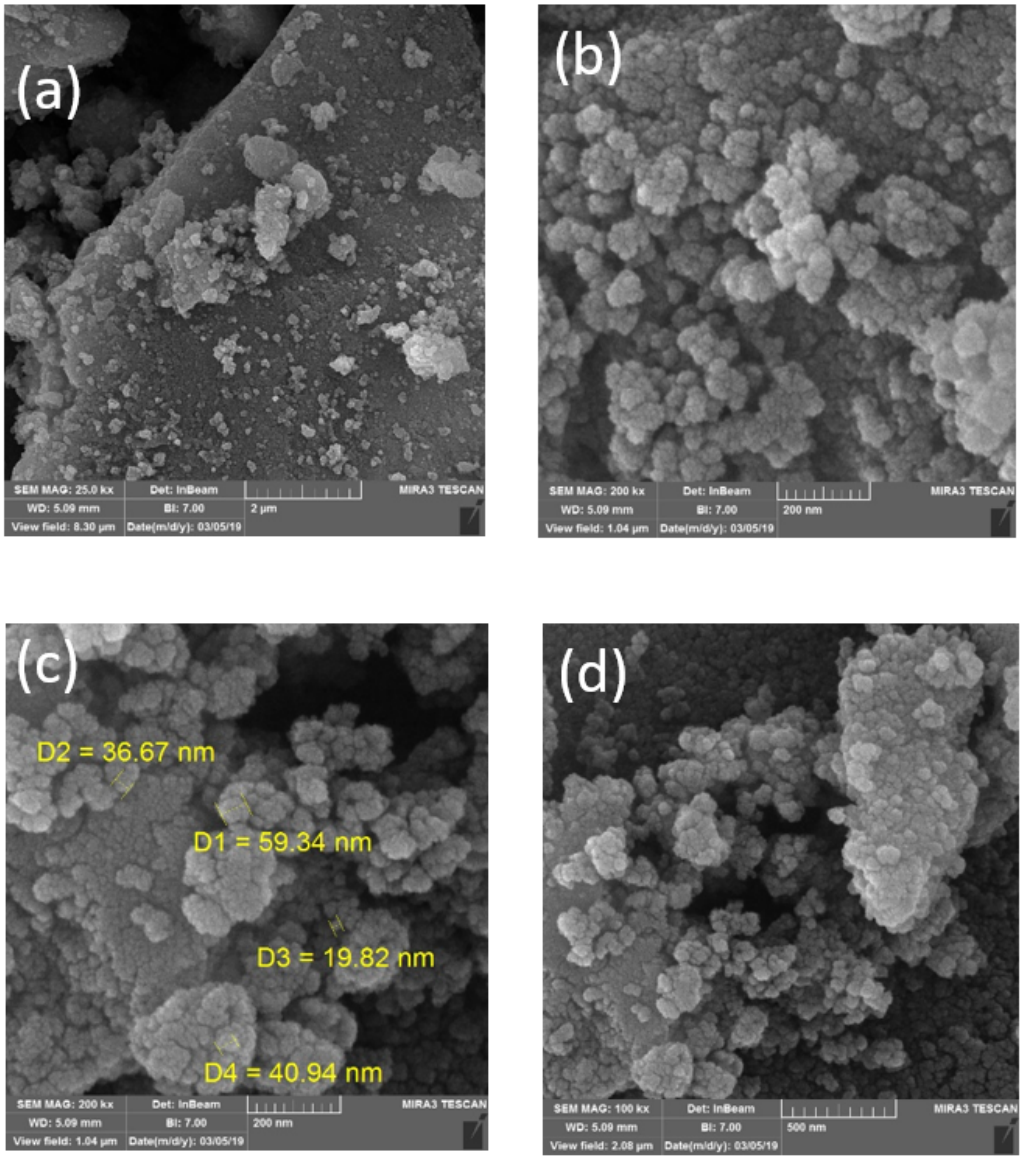

Figure 5

FESEM images of the Fe_3O_4@SiO_2@PTS-APG catalyst.

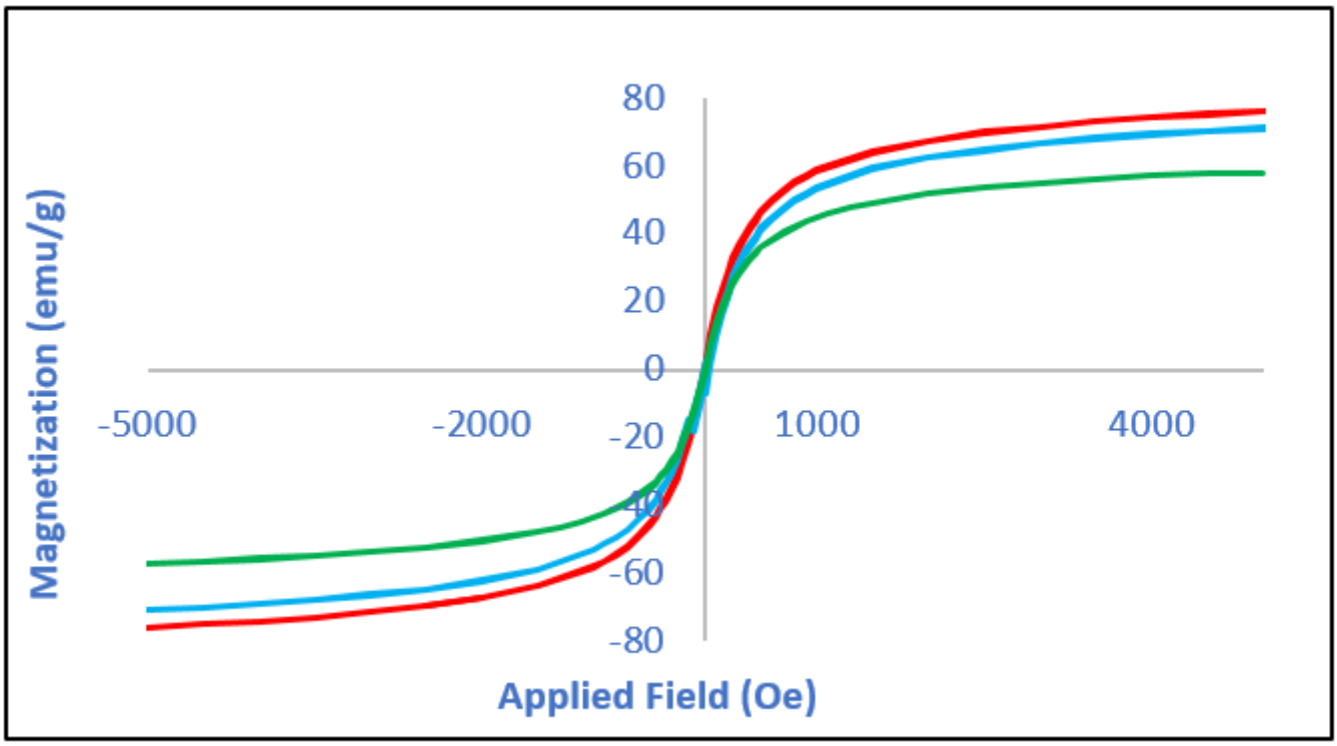

Figure 6

Magnetization curves of the (red) Fe_3O_4, (blue) Fe_3O_4@SiO_2 and (green) Fe_3O_4@SiO_2@PTS-APG MNPs.

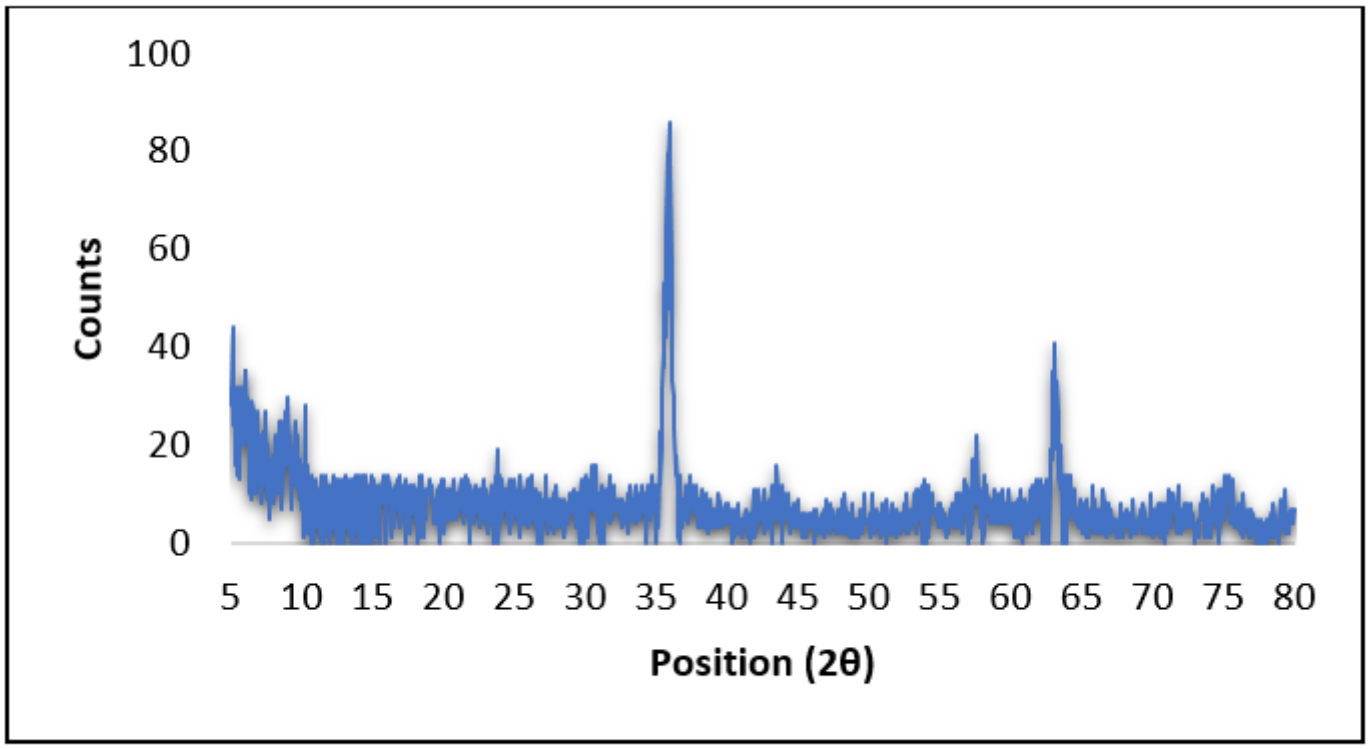

Figure 7

XRD Pattern of the Fe_3O_4@SiO_2@PTS-APG nanocatalyst.

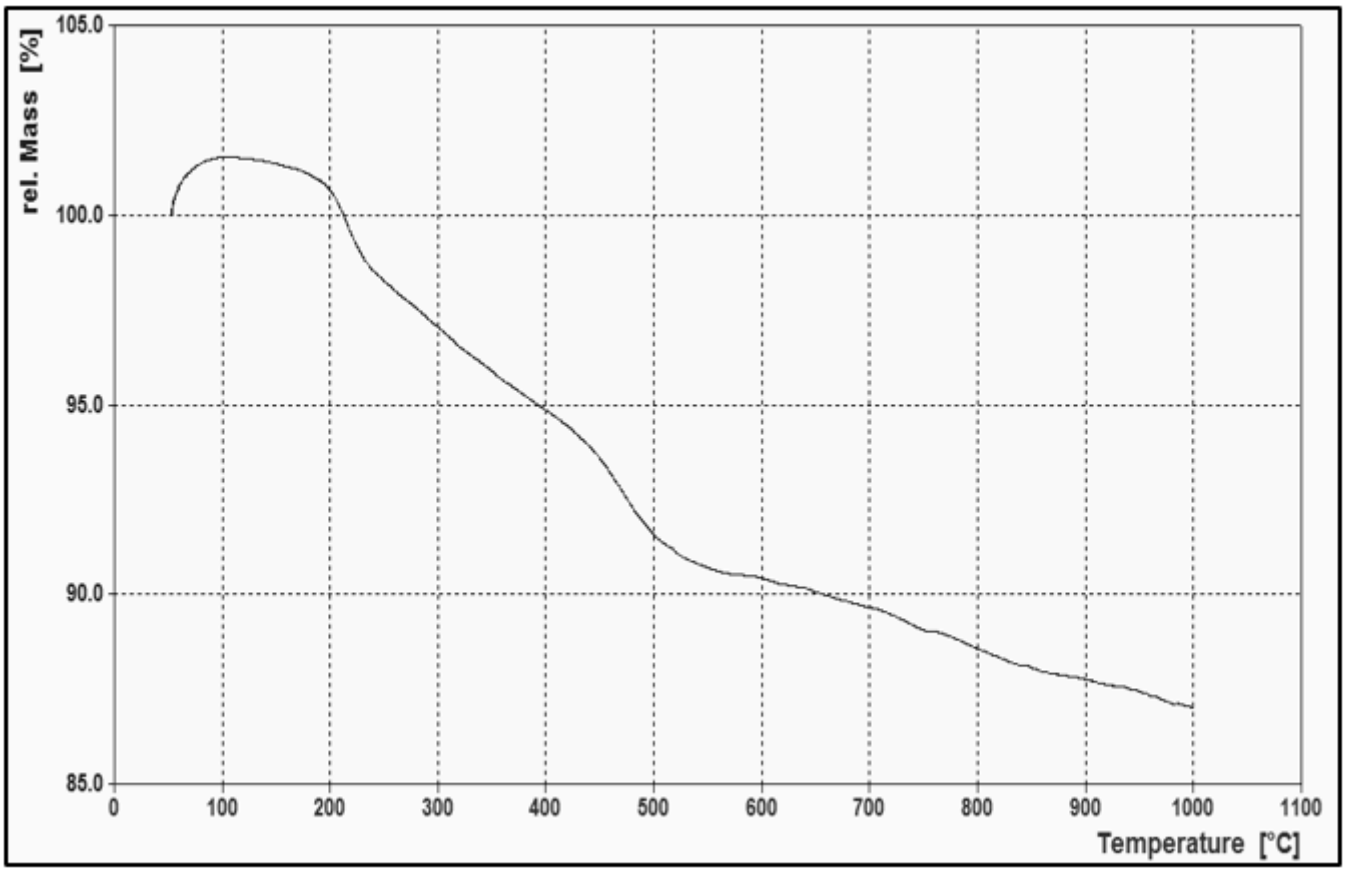

Figure 8

TGA curve of the Fe_3O_4@SiO_2@PTS-APG.

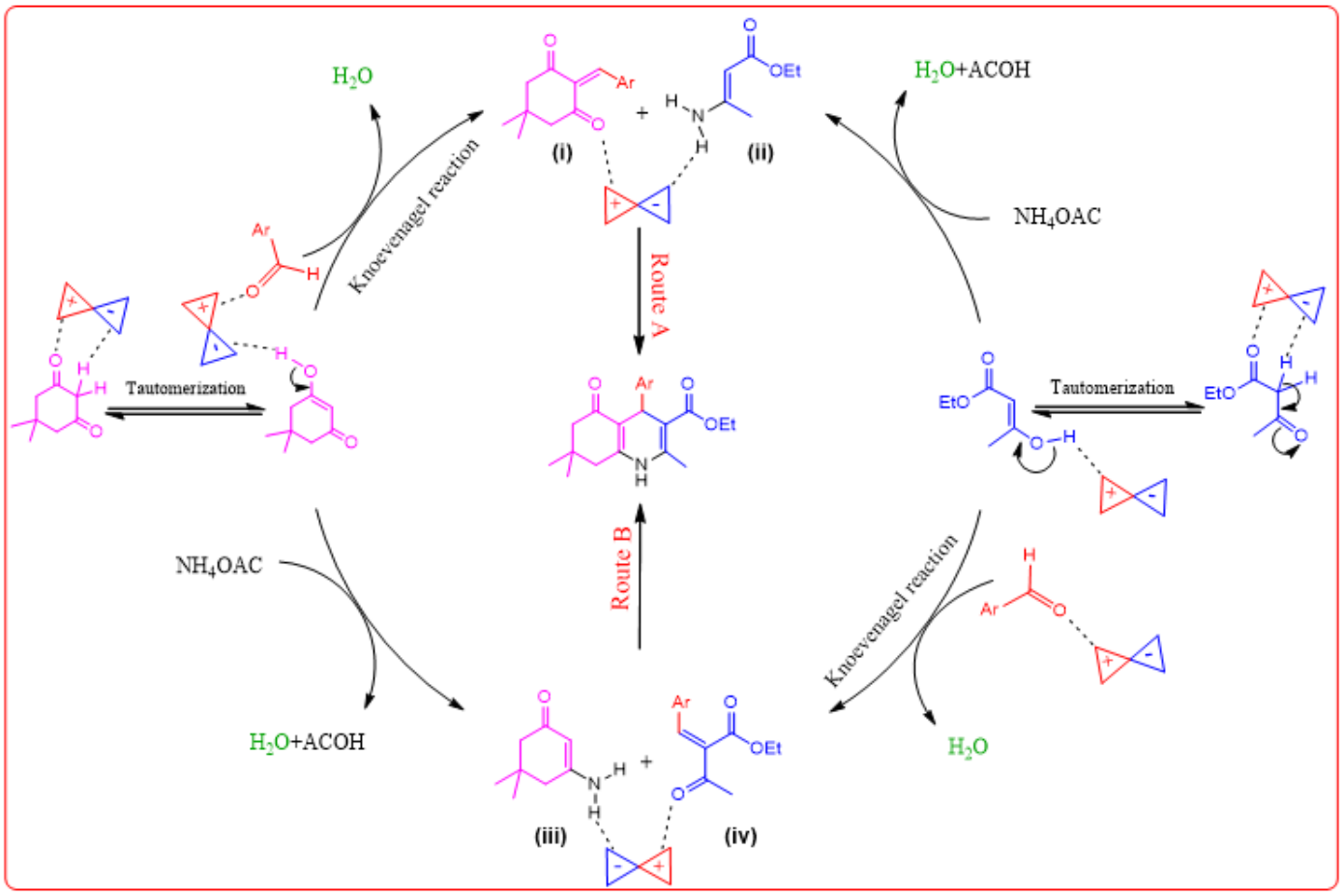

Figure 9

A proposed mechanism for the synthesis of polyhydroquinoline catalyzed by the Fe_3O_4@SiO_2@PTS-APG MNPs.

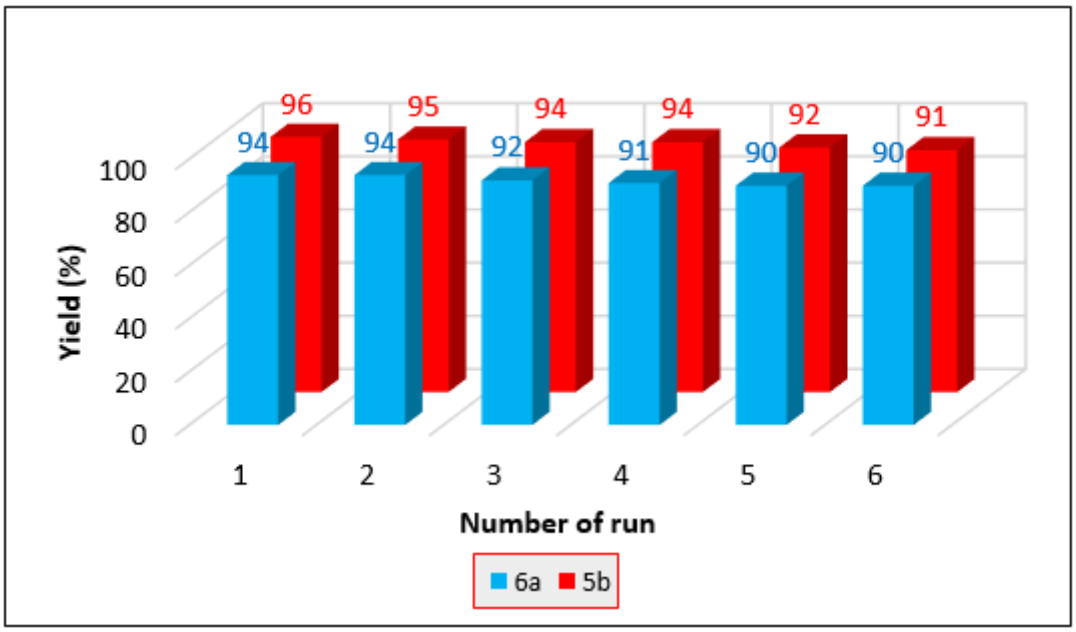

Figure 10

Reusability of the Fe_3O_4@SiO_2@PTS-APG MNPs in the synthesis of **5b** (red) and **6a** (blue) under optimized conditions.

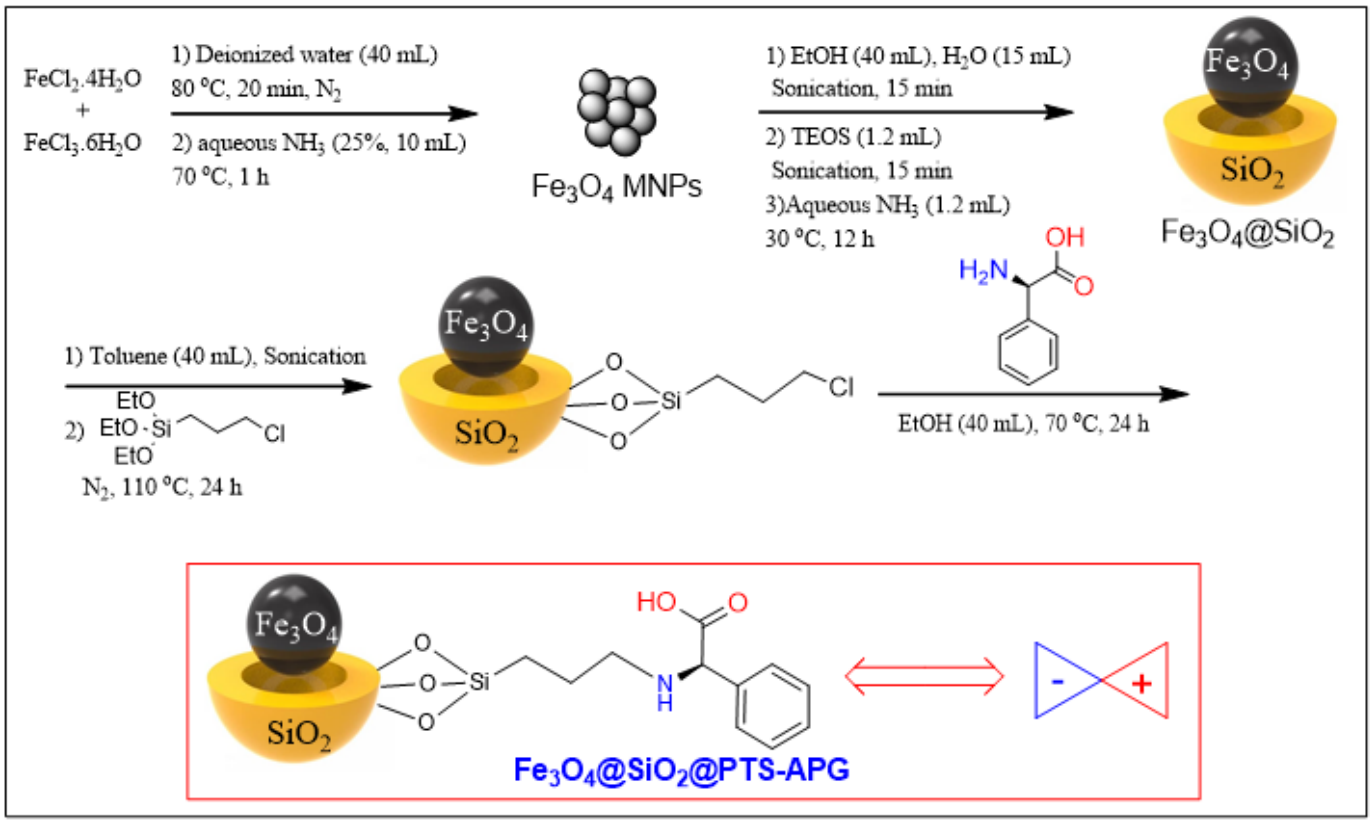

Figure 11

Schematic preparation of the Fe_3O_4@SiO_2@PTS-APG nanocatalyst.

Supplementary Files

This is a list of supplementary files associated with this preprint. Click to download.

- Table1to6.docx
- ESIScienificReports.docx